

NJC

Accepted Manuscript



This is an *Accepted Manuscript*, which has been through the Royal Society of Chemistry peer review process and has been accepted for publication.

Accepted Manuscripts are published online shortly after acceptance, before technical editing, formatting and proof reading. Using this free service, authors can make their results available to the community, in citable form, before we publish the edited article. We will replace this *Accepted Manuscript* with the edited and formatted *Advance Article* as soon as it is available.

You can find more information about *Accepted Manuscripts* in the [Information for Authors](#).

Please note that technical editing may introduce minor changes to the text and/or graphics, which may alter content. The journal's standard [Terms & Conditions](#) and the [Ethical guidelines](#) still apply. In no event shall the Royal Society of Chemistry be held responsible for any errors or omissions in this *Accepted Manuscript* or any consequences arising from the use of any information it contains.



www.rsc.org/njc

ARTICLE

Surface activation of cotton fiber by seeding silver nanoparticles and in situ synthesizing ZnO nanoparticles

Cite this: DOI: 10.1039/x0xx00000x

Received 00th January 2012,
Accepted 00th January 2012

DOI: 10.1039/x0xx00000x

www.rsc.org/

Hossein Barani

The paper describes the study of photocatalytic oxidation and antibacterial properties of cotton fabric treated with zinc oxide/silver (ZnO/Ag) nanocomposites. The ZnO nanoparticles were synthesized by an in situ approach on the surface of activated cotton fibers with seeded Ag nanoparticles. The effect of Ag nanoparticles seeding and synthesis temperature on the morphological, thermal, photocatalytic and antibacterial properties of ZnO/Ag nanocomposites treated cotton fibers were characterized using scanning electron microscopy, energy dispersive X-ray spectroscopy, X-ray diffractometer, thermo gravimetric analysis, Attenuated Total Reflection-Fourier Transform Infrared spectrometer. Synthesizing ZnO nanoparticles on the surface of un-activated cotton fibers lead to the formation of agglomerated nanoparticles while the Ag nanoparticles seeded cotton fibers prevented forming the same. The results indicated the presence of ZnO/Ag nanocomposites on the coated cotton fabrics, and all loaded samples presented an inhibition zone against *S. aureus* and *E. coli* bacteria.

Introduction

Cotton fibers are very popular and people widely use them in daily life due to its softness, affinity to the skin, sweat absorbing properties, etc. However, cotton fibers can be easily damaged by microbial attack and ultraviolet radiation. The microbial attack of the fibers leads to an enhanced discoloration, decomposition and mechanical strength loss with time¹⁻⁴. There are several methods to modify the surface of cotton to overcome the above-mentioned problems. Moreover, the use of nanotechnology in the textile industry has increased rapidly as a result of its unique properties which can produce multifunctional fibers with variable functions and applications such as antimicrobial, UV protection, self-cleaning, etc. Several nanoparticles with various sizes and structures have been fabricated and fixed on fibers to produce multifunctional textile products⁵.

Zinc oxide (ZnO) is a semiconductor with a large binding energy and wide-band gap⁶. ZnO nanoparticles are a well-known coating material used to improve the functionality of textile products. They are used for a wide range of applications due to their unique photocatalytic, electrical, optical and antibacterial properties⁷⁻⁹. Two different approaches have been proposed to immobilize these nanoparticles on the surface of textile fibers. The first type of approach is coating the surface of fibers with pre-synthesized nanoparticles. This approach consists of two steps: first, the synthesis of nanoparticles and second, the immobilization on the surface of fibers¹⁰. The second type of approach is to directly synthesis nanoparticles on the surface of fibers, which is known as

an in situ method and this is without the pre-synthesis step^{4, 11, 12}. In this method, metal ions are attached onto fibers via electrostatic adsorption or ion exchange, and this is followed by a reduction step to produce nanoparticles. The facile in situ synthesis approach could provide strong binding between nanoparticles and the fibers¹³.

Hybrid semiconductor nanocomposite materials are attractive candidates for advanced nanoparticles due to synergies between different components¹⁴ and these can display novel physical and chemical properties¹⁵. Metal-semiconductor nanoparticles have been extensively studied due to their excellent catalytic activity. Ag-ZnO heterogeneous nanostructures were synthesized with a seed-mediated method¹⁶. The well-defined faceted nanoparticles are prepared as seeds and mixed with a metal salt precursor in the presence of suitable surfactants. The seeds act as efficient catalysts, which then occur selectively at their surface. More recently, Ag-ZnO hybrid nanoparticles are synthesized with a hexagonal pyramid-like structure by a seed-mediated method. The growth mechanism is attributed to a good lattice and symmetry match between ZnO and Ag in the corresponding planes¹⁷. In addition, it is reported that the antibacterial properties of Ag-ZnO nanohybrid on Gram-positive and Gram-negative bacteria are better compared to the individual components (ZnO and Ag)¹⁸.

The aim of this work was to use in situ approach to synthesize ZnO/Ag nanocomposites on the surface of cotton fibers. The surface of cotton fibers were, firstly, activated with Ag nanoparticles (AgNPs) as seeds, then the ZnO nanoparticles was synthesized on these activated cotton fibers. The morphological property of cotton fabrics was observed by scanning electron microscopy (SEM) which

was equipped with Energy Dispersive X-ray spectroscopy (EDS). The chemical property of coated cotton fabric was analyzed with Attenuated Total Reflection-Fourier Transform Infrared spectrometer (ATR-FTIR). Thermal characteristics and antibacterial properties of coated samples were also evaluated.

Experimental

Chemical agents

All chemical agents were used in this study were of analytical grade. Distilled water was used throughout the work. Zinc acetate dihydrate ((CH₃COO)₂Zn, 2H₂O), sodium hydroxide (NaOH, 99.9%), tin chloride (SnCl₂), hydrochloric acid (HCl), silver nitrate (AgNO₃, extra pure), ammonia (NH₃, 25%), sodium hypophosphite (NaPO₂H₂), and citric acid (C₆H₈O₇) was purchased from Merck Co (Germany).

A plain-woven cotton fabric (100%) with a mass per unit area of 240 g m⁻² was used in this study. All cotton samples were scoured with a Triton X 100 (1 g L⁻¹), nonionic surfactant that has a hydrophilic polyethylene oxide chain (C₁₆H₂₅O)₃₀OH, for 30 min at 60°C (L:G = 40:1), then rinsed with tap water and immersed in a acetone solution for 15 min. These samples were then dried at room temperature.

Activation of cotton surface by seeding silver nanoparticles

The surface of cotton fibers was activated by deposition of silver nanoparticles on their surface by in situ synthesizing method. For the sensation step, a scoured cotton sample was immersed into the sensation solution (L: G of 50:1) which was composed of SnCl₂ solution (Wt%, 2%), and HCl (Wt%, 1%) at 25 °C for 30 minutes. At the activation step, the sample was introduced into a solution of AgNO₃ (L: G of 50:1) which contained Ag ions (Wt%, 0.5%), and NH₃ (Wt%, 0.25%) at 25 °C for 30 minutes. Silver ions were converted to the silver nanoparticles in the presence of tin chloride which acted as a reducing agent. Seeding silver nanoparticles on the surface of cotton fibers result in activation of cotton surface.

Synthesizing ZnO nanoparticles

The cotton fibers act as a template for the growth ZnO nanoparticles. The cotton sample was introduced into a solution (L: G of 50:1) containing (CH₃COO)₂Zn, 2 H₂O (0.09 M), NaPO₂H₂ (0.015 M), C₆H₈O₇ (0.065 M) and treated at 25°C for 30 min at this solution. The treatment was followed for 30 min at the proposed temperatures at Table1. After that, this sample was introduced into the NaOH solution with twice the molar concentration at the same temperature of previous step for 45 min and then rinsed with distilled water.

Characterization

The surface morphologies of all cotton fabrics were observed by scanning electron microscopy (SEM) (Philips XL 30). Cotton fabrics were coated with gold in a sputter coating unit for 5minutes before SEM observation. For the analysis, qualitative and quantitative elemental composition of samples, Energy Dispersive X-ray spectroscopy (EDS) was used.

Thermo gravimetric analysis (TGA) of all cotton fabrics was performed with a Perkin-Elmer 7 thermal analyzer. For this purpose, a weighed fabric sample (roughly 7 mg) was heated from 25°C to 650°C with heating rate of 10 °C min⁻¹ in the presence of nitrogen gas.

Table 1 Description of sample code and their preparation conditions

Sample code	Description
Activated-AgNPs	Activated sample by seeding silver nanoparticles
ZnO-coated	In situ synthesized ZnO nanoparticles on un-activated sample
Ag-ZnO-T70	In situ synthesized ZnO nanoparticles on the activated sample at 70°C
Ag-ZnO-T25	In situ synthesized ZnO nanoparticles on the activated sample at 25°C

In order to explore chemical interactions at the surface of coated cotton fabrics Attenuated Total Reflection-Fourier Transform Infrared spectrometer (ATR-FTIR, Perkin Elmer Spectrum 100 series) was used. The spectra were recorded at a resolution of 1cm⁻¹ and the scanning range was 650–4000 cm⁻¹ and an average of 20 scans was recorded.

The structure of synthesized nanoparticles was analyzed with X-ray diffraction (XRD) measurements and performed on INEL EQuinox 3000 X-ray diffractometer over the range of 2θ = 10° to 90°.

The antibacterial efficiency of treated cotton fabrics was carried out according to AATCC test method 147-2004. The test was done with *Staphylococcus aureus* ATCC 6538 (Gram-positive) and *Escherichia coli* ATCC 8739 (Gram-negative bacterium). The antibacterial efficiency was calculated according to equation (1):

$$W = \frac{T-D}{2} \quad (1)$$

Where W is the inhibition zone width in mm, and T is the total diameter of test specimen and clear zone, and D is the diameter of the test specimen.

Photo degradation property of the samples was determined by staining the fabrics with a drop (Approximately 0.05 ml) of 0.5,Wt% Methylene Blue. The stained samples were exposed to Light (MH-BT, 400W E40) irradiation for 12 h. The color difference of stained sample after irradiated time was calculated according to equation (2):

$$\Delta E = \sqrt{(L_a - L_b)^2 + (a_a - a_b)^2 + (b_a - b_b)^2} \quad (2)$$

Where the L, a, and b are the color-coordinates of the sample a, and b indices to present after and before irradiation.

Results and discussion

The ZnO nanoparticles were grown on the surface of activated and un-activated cotton fiber at different temperature. The

cotton fibers act as a template for the growth of ZnO nanoparticles and were activated with seeding silver nanoparticles on their surface. The SEM images of treated cotton fibers with nanoparticles are presented in Fig. 1. The surface morphology of cotton fibers loaded with nanoparticles was changed. The presence of nanoparticles is clearly seen. The cotton fibers were activated with AgNPs resulted in formation AgNPs seeds on the surface of cotton fibers (Fig. 1a). Loading ZnO nanoparticles into the un-activated cotton fibers lead to the formation of agglomerated nanoparticles on the surface of cotton fiber (Fig. 1b). Activation with AgNPs prevented the formation of agglomerated ZnO nanoparticles on the surface of cotton fibers. Deposition of ZnO nanoparticles at 70 °C on the cotton fabrics resulted in the surface being covered with a dense layer of ZnO nanoparticles, but the deposited surface of cotton fibers appeared rougher¹⁹. The reaction temperature increased the deposition rate of ZnO nanoparticles on the surface of cotton fabric. Increase in temperature of ZnO synthesizing step resulted formation of partially agglomerated nanoparticles on the surface compared to the sample synthesized at lower temperature (Fig. 1c, and 1d).

The EDS spectra of cotton fabrics loaded with nanoparticles is shown in Fig. 2. The characteristic peaks of Ag nanoparticles appeared around 2.91, 3.41, 22.12, and 24.95 keV (Fig. 2a).

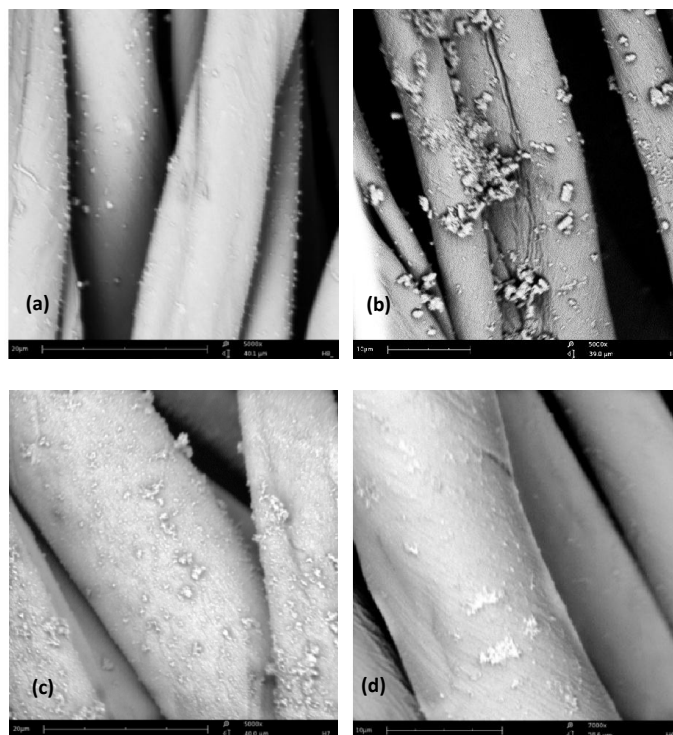


Fig. 1 SEM images of loaded cotton fibers a) Activated-AgNPs, b) ZnO-coated, c) Ag-ZnO-T70, d) Ag-ZnO-T25

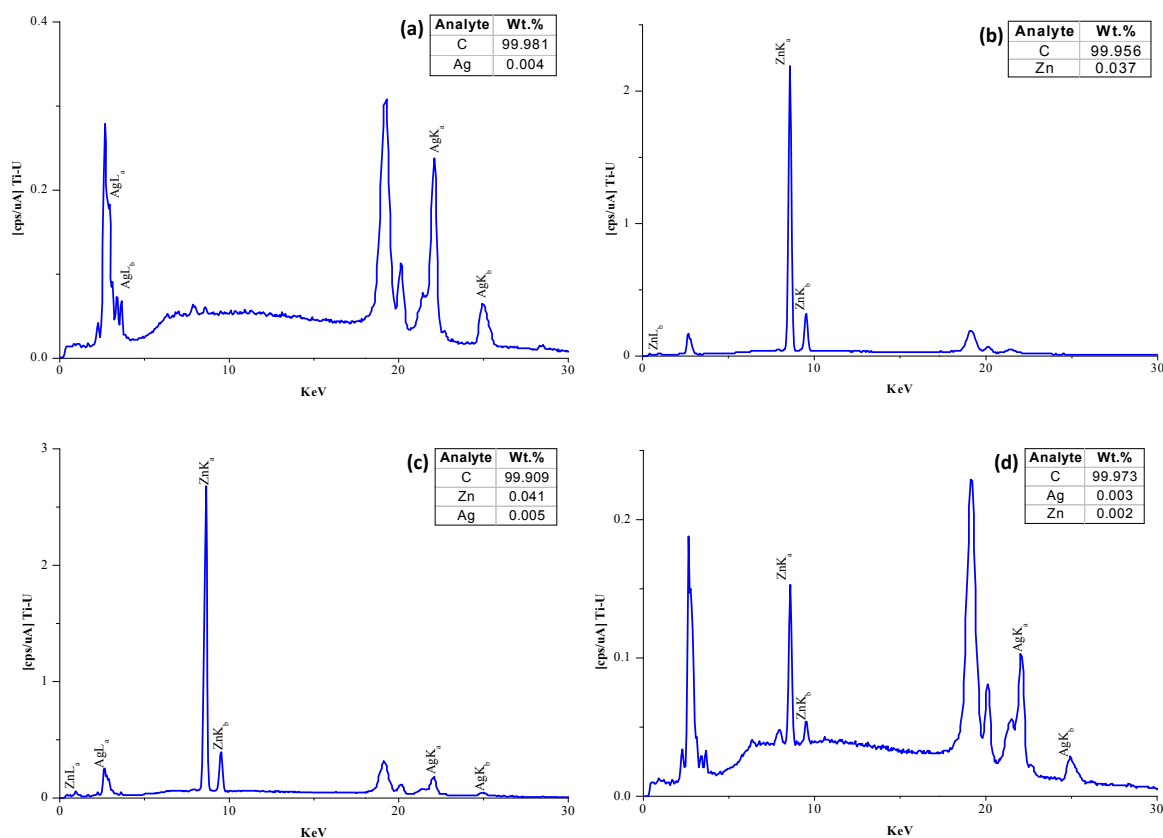


Fig. 2 EDS spectra of loaded cotton fibers a) Activated-AgNPs, b) ZnO-coated, c) Ag-ZnO-T70, d) Ag-ZnO-T25

Peaks appeared at about 0.98, 8.6, and 9.6 keV and these correspond to that of Zn (Fig. 2b). This confirms the presence of ZnO/Ag nanoparticles on the activated cotton fabrics. In addition, these results also indicated that the Ag-ZnO-T70 sample has the highest amount of Zn (Fig. 2c). However, Ag activation and subsequent loading with ZnO nanoparticles at 25°C did not lead to a higher amount of ZnO nanoparticles on the surface of cotton fabric (Fig. 2.d). Therefore it was deduced that the Ag activation step and temperature of ZnO synthesis influence the loading efficiency.

The results of thermal characteristic study of cotton fabrics are presented in Table 2. The decomposition and thermal stability of cotton fabrics have been evaluated by thermo gravimetric analysis. These tests were done in inert condition. Fig. 3 shows the TGA curves of pristine and loaded cotton fabrics. The thermal degradation of all samples proceeds by a one stage reaction process between 200 and 500 °C. The reaction is characterized by T_i that is the lowest temperature at which the onset of a mass change can be detected. Anticipation in the degradation process of all loaded cotton fabrics can be seen (see inset of Fig. 3) and reduced T_i of loaded samples to a lower temperature compare to the pristine samples (Table 2). There is a mass loss at the first stage of TG curves (see inset Fig. 3) which is due to the moisture evaporation of cotton fabrics. Loading cotton fabrics with nanoparticles leads to increase in the moisture content of cotton fabric. The activated cotton fabric with AgNPs (Activated-AgNPs) presented the highest moisture content (7%).

Table 2 The thermal properties, moisture content, and residual weight of cotton fabrics

Sample	T_i (°C)	Moisture content%	Residual weight at 650 °C (%)
Pristine	307.05	4.87	9.10
Activated-AgNPs	293.18	7.07	13.13
ZnO-coated	235.13	6.98	22.31
Ag-ZnO-T70	241.13	5.22	25.90
Ag-ZnO-T25	281.47	6.02	14.24

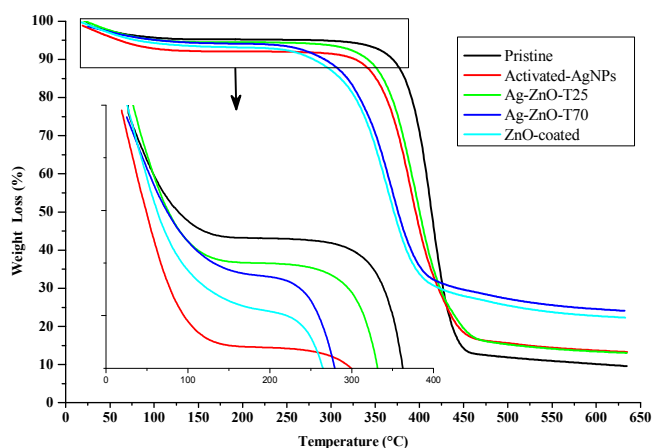


Fig. 3 TGA curves of pristine and coated cotton fabric with AgNPs and ZnO/Ag nanocomposites

There is a significant increase in the residual weight of loaded cotton fabrics with nanoparticles compared to the pristine cotton sample. The residual weight of Ag-ZnO-T70 and ZnO-coated samples at 650 °C is about 25.9, and 22.31% respectively and this is due to the fact that the Ag activation step resulted in higher loading of ZnO nanoparticles into the cotton fabric. The Ag-ZnO-T25 sample presents a residual weight of 14.24% that is lower compared to ZnO content of Ag-ZnO-T70 sample. Therefore, the loading temperature of ZnO has a significant effect on the loading content of ZnO into the cotton fabric.

The ATR-FTIR spectra of pristine cotton fabric and loaded with ZnO nanoparticles in 600-4000 cm^{-1} region are presented in Fig. 4. The spectra of cotton fabrics were normalized against the 1317 cm^{-1} band, which is associated with the C-H bending vibration mode of cellulose molecules²⁰. The absorption bands in the 900-1300 cm^{-1} and 1300-1500 cm^{-1} region are associated to C-O and C-H vibration, which are the characteristic peaks of cellulose fiber and observed in all spectra of cotton fabrics²¹. The loaded cotton fabric with ZnO nanoparticles presented a new absorption band around at 1568 cm^{-1} (see inset Fig. 4) which represent the carboxylate carbonyl of the free carboxylic of citric acid²². A broad absorption band was centred in 3330 and 2895 cm^{-1} which are associated to hydrogen bonded O-H stretching in cellulose molecules²³. Loaded cotton fabric with ZnO nanoparticles led to reduce the intensity of these bands which confirm replacement of the O-H groups of the cellulose by the ZnO nanoparticles²⁴ (Fig. 4).

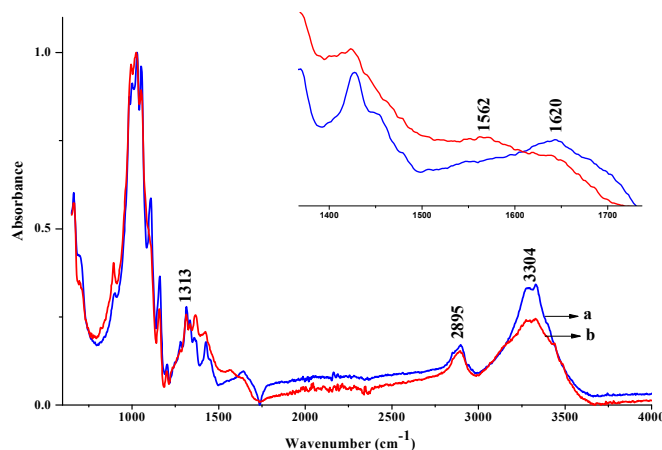


Fig. 4 ATR-FTIR spectra of: a) pristine cotton fabric, b) cotton fabric loaded with ZnO nanoparticles (Ag-ZnO-T70)

The X-ray diffraction spectra of cotton fabrics are presented in Fig. 5. Cotton fibers as same as a semi crystalline polymer structure presented some large and wide reflections due to its internal structure and can be assigned according to the literature^{25, 26}. The characteristic peaks of cellulose structure were appeared in all untreated and loaded samples with nanoparticles near to the 2θ angles of 14.8°, 16.8°, 22.2°, and 34.1°, which are associated to (101), (101), (002), and (040). Moreover, the cotton fabric loaded with nanoparticles present some different characteristic peaks (see inset Fig. 5) at the wide angle X-ray diffraction spectra near to 2θ angles of 31.8°, 34.4°, 36.2°, and 56.6° and are associated to (100), (002), (101), (102), (110), and (103) due to presence of ZnO nanoparticles. Another new peak, due to presence of Ag nanoparticles, appeared at the 2θ angles of 38.7° and this is related to (111) plane of the face-

centered cubic structure of the AgNPs¹³. The Ag-ZnO-T70 sample shows higher intensity for these new peaks compared to Ag-ZnO-T25 sample and this is due to the higher nanoparticles content. Due to the position of these new peaks, it can be concluded that the synthesized ZnO particles have a hexagonal wurtzite crystal structure²⁷. The hexagonal plates of ZnO nanoparticles have (001) polar planes and (110) non-polar planes and later planes are parallel and perpendicular to the c axis respectively. The polar planes have a higher photocatalytic activity than the non-polar planes²⁸. The ratio intensity of (002) and (110) of Ag-ZnO-T25 and Ag-ZnO-T70 samples is 2.99 and 2.49 respectively. Therefore, in the Ag-ZnO-T25 sample, the proportion of the (002) polar plane is higher compared to the (110) non-polar plane of the hexagonal plates.

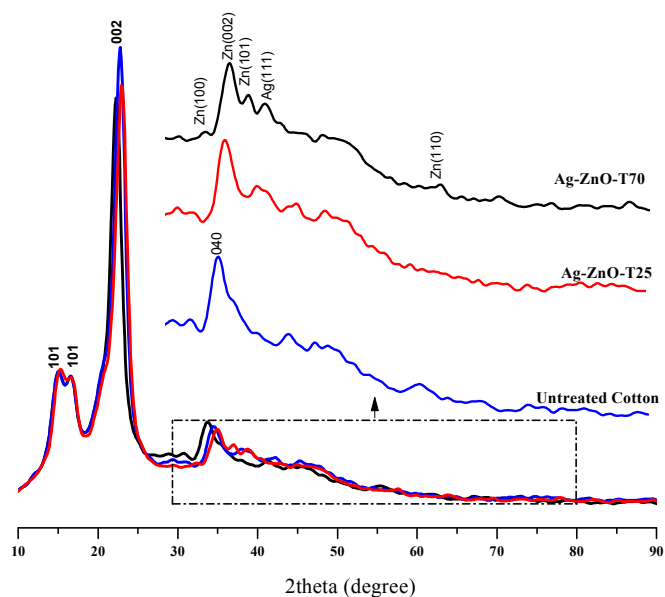


Fig. 5 Wide-angle X-ray diffraction pattern of cotton fabrics loaded with ZnO nanoparticles

The loading of nanoparticles into the cotton fibers act as a barrier and control the rate of bacterial proliferation. ZnO nanoparticles loaded are of great interest in regard to their antimicrobial activity⁵. ZnO nanoparticles generate reactive oxygen species which lead to bacterial cell membrane destruction and thereby result in a decrease in the bacterial population²⁹. The mean value of the inhibition zone of all cotton fabrics is reported in Table 3. There was no inhibition zone around the untreated cotton fabric against the two types of test bacteria. The antibacterial activity of cotton fabrics loaded with ZnO nanoparticles is obvious from the clear zone of the inhibition zone around the sample where no bacterial growth is observed. The width of the inhibition zone is larger against *S. aureus* than the *E. coli*. The Ag-ZnO-T70 and Ag-ZnO-T25 have the highest and lowest width of the inhibition zone respectively and these are related to the ZnO content of these samples. In addition, ZnO-coated sample presented a lower antibacterial property compared to the Ag-ZnO-T70 sample due to the structure of ZnO synthesized nanoparticles and their content in the Ag-ZnO-T70 sample. It can be concluded that stabilized and uniform structure of ZnO nanoparticles present better antibacterial properties.

The photocatalytic oxidation properties of ZnONPs-loaded samples after 12h irradiation as means of color differences (ΔE) of stained fabric are presented in Table 4. The color-coordinate difference is calculated taking the colour values before and after irradiation of stained cotton fabrics. Metal oxides present the photo-oxidizing and photocatalytic properties due to the donor states of defect locations such as oxygen vacancies as well as the interstitial atoms of zinc and oxygen³⁰. The ZnO nanoparticles present the photocatalytic activity in comparison to TiO₂ under the visible-light illumination. The photocatalytic activity of ZnO nanoparticles depends on their morphology³¹, the ratio intensity of polar to nonpolar planes, and polar planes have a higher photocatalytic activity²⁸. The Ag-ZnO-T25 sample with the highest ratio intensity of polar to nonpolar planes shows the highest photocatalytic oxidation activity and higher photo degradation.

Table 3 Mean width value of the inhibition zone around of cotton fabrics

Sample	Bacterial strain	<i>S. aureus</i>	<i>E. coli</i>
		Inhibition zone (mm)	
Untreated cotton fabric		0	0
ZnO-coated		3.25	1
Ag-ZnO-T25		1	0.25
Ag-ZnO-T70		5.5	1.25

Table 4 Color differences of unloaded and loaded cotton fabrics with nanoparticles

Sample	ΔE
Untreated cotton fabric	5.19
Activated-AgNPs	9.26
ZnO-coated	29.52
Ag-ZnO-T25	35.24
Ag-ZnO-T70	22.32

Conclusion

The Ag nanoparticles seeded cotton fibers resulted in prevent an agglomeration of ZnO nanoparticles, while the synthesis of ZnO nanoparticles on the un-activated cotton fibers led to the formation of agglomerated nanoparticles. In addition, increasing the temperature during the synthesis of ZnO allows the formation of partially agglomerated nanoparticles. The EDS and TGA results indicated that the Ag nanoparticles seeding and temperature of reaction deposition influence on the ZnO content and Ag-ZnO-T70 sample has the highest amount of Zn. Loading cotton fabric with nanoparticles led to an increase in the moisture content of cotton fabric and activated cotton fabric with AgNPs (Activated-AgNPs) showed highest moisture content (7%). A clear inhibition zone appeared around the cotton fabric loaded with ZnO nanoparticles. The width of the inhibition zone in samples treated with ZnO nanoparticles is larger against *S. aureus* than the *E. coli*. The Ag-ZnO-T70 and Ag-ZnO-T25 have the highest and lowest width of the inhibition zones. This is related to the ZnO content of these samples.

Notes and references

Faculty of Art, University of Birjand, 17 shahrivar street, Birjand, Iran,
Email: Barani@birjand.ac.ir; Phone: +98 561 2502050; Fax: +98 561 2227225

1. A. El-Shafei and A. Abou-Okeil, *Carbohydrate Polymers*, 2011, **83**, 920-925.
2. A. Haji, H. Barani and S. S. Qavamnia, in *Micro & Nano Letters*, Institution of Engineering and Technology, 2013, vol. 8, pp. 315-318.
3. A. Haji, H. Barani and S. S. Qavamnia, *INDUSTRIA TEXTILA*, 2013, **64**, 8-12.
4. H. Barani, M. Montazer, N. Samadi and T. Toliyat, *Colloids and Surfaces B: Biointerfaces*, 2012, **92**, 9-15.
5. R. Dastjerdi and M. Montazer, *Colloids and Surfaces B: Biointerfaces*, 2010, **79**, 5-18.
6. M. K. Debanath and S. Karmakar, *Materials Letters*, 2013, **111**, 116-119.
7. R. Zou, G. He, K. Xu, Q. Liu, Z. Zhang and J. Hu, *Journal of Materials Chemistry A*, 2013, **1**, 8445-8452.
8. C. Rimbu, N. Vrinceanu, G. Broasca, C. Campagne, M. P. Sucheai and A. Nistor, *Textile Research Journal*, 2013.
9. H.-M. Xiong, *Journal of Materials Chemistry*, 2010, **20**, 4251-4262.
10. R. Dastjerdi and M. Montazer, *Colloids and Surfaces B: Biointerfaces*, 2011, **88**, 381-388.
11. H. Barani, M. Montazer, A. Calvimontes and V. Dutschk, *Textile Research Journal*, 2013, **83**, 1310-1318.
12. Q. Shi, N. Vitichuli, J. Nowak, J. Noar, J. M. Caldwell, F. Breidt, M. Bourham, M. McCord and X. Zhang, *Journal of Materials Chemistry*, 2011, **21**, 10330-10335.
13. Z. Lu, M. Meng, Y. Jiang and J. Xie, *Colloids and Surfaces A: Physicochemical and Engineering Aspects*, 2014, **447**, 1-7.
14. C. d. M. Donega, *Chemical Society Reviews*, 2011, **40**, 1512-1546.
15. H. Park, S. Chang, J. Jean, J. J. Cheng, P. T. Araujo, M. Wang, M. G. Bawendi, M. S. Dresselhaus, V. Bulović, J. Kong and S. Gradečak, *Nano Letters*, 2012, **13**, 233-239.
16. F.-R. Fan, Y. Ding, D.-Y. Liu, Z.-Q. Tian and Z. L. Wang, *Journal of the American Chemical Society*, 2009, **131**, 12036-12037.
17. J. Zhang, W. Wang and X. Liu, *Materials Letters*, 2013, **110**, 204-207.
18. S. Ghosh, V. S. Goudar, K. G. Padmalekha, S. V. Bhat, S. S. Indi and H. N. Vasani, *RSC Advances*, 2012, **2**, 930-940.
19. N. Preda, M. Enculescu, I. Zgura, M. Socol, E. Matei, V. Vasilache and I. Enculescu, *Materials Chemistry and Physics*, 2013, **138**, 253-261.
20. A. Budimir, S. Bischof Vukusic and S. Grgac Flincec, *Cellulose*, 2012, **19**, 289-296.
21. Yongliang Liu, D. Thibodeaux and G. Gamble, *Textile Research Journal*, 2011, **81**, 1559-1567.
22. C. Q. Yang, *Textile Research Journal*, 1993, **63**, 706-711.
23. K. Ghule, A. V. Ghule, B.-J. Chen and Y.-C. Ling, *Green Chemistry*, 2006, **8**, 1034-1041.
24. M. Periolatto, F. Ferrero, A. Montarsolo and R. Mossotti, *Cellulose*, 2013, **20**, 355-364.
25. S. Gordon, Y. L. Hsieh and T. Institute, *Cotton: Science and Technology*, Woodhead Publishing, 2007.
26. H. F. Moafi, A. F. Shojaie and M. A. Zanjanchi, *Thin Solid Films*, 2011, **519**, 3641-3646.
27. D. Bhardwaj, P. Sharma and P. S. Khare, *Materials Letters*, 2013, **111**, 134-136.
28. D. M. Lewis, S. o. Dyers and Colourists, *Wool Dyeing*, Society of Dyers and Colourists, 1992.
29. P. Dhandapani, A. S. Siddarth, S. Kamalasekaran, S. Maruthamuthu and G. Rajagopal, *Carbohydrate Polymers*, 2014, **103**, 448-455.
30. M. Montazer and M. Maali Amiri, *The Journal of Physical Chemistry B*, 2013.
31. T.-J. Liu, Q. Wang and P. Jiang, *RSC Advances*, 2013, **3**, 12662-12670.